Transcriptome analysis revealed the potential mechanism of a wheat-Th. elongatum translocation line YNM158 against Fusarium head blight

Yi Dai
Yangzhou University
Wenlin Fei
Yangzhou University
Shiqiang Chen
Institute of Agricultural Sciences for Lixiahe Region in Jiangsu
Juntao Shi
Yangzhou University
Haigang Ma
Yangzhou University
Haifeng Li
Yangzhou Polytechnic College
Jinfeng Li
Yangzhou University
Yonggang Wang
Yangzhou University
Yujiao Gao
Yangzhou University
Jinghuan Zhu
ZheJiang Academy of Agricultural Sciences
Bingkui Wang
ZheJiang Academy of Agricultural Sciences
Jianmin Chen
Yangzhou University
Hongxiang Ma
mahx@yzu.edu.cn

Yangzhou University

Research Article

Keywords: Fusarium head blight, wheat-Th. elongatum translocation line, transcriptome analysis, disease resistance pathway

Posted Date: March 27th, 2024

DOI: https://doi.org/10.21203/rs.3.rs-4079736/v1

Additional Declarations: No competing interests reported.

Abstract

Background

Fusarium head blight (FHB) caused by *Fusarium graminearum* species complex is a destructive disease in wheat worldwide. Lack of FHB resistant germplasm is a barrier in wheat breeding for the resistance to FHB. *Thinopyrum elongatum* is an important relative species successfully used for genetic improvement in wheat.

Results

In this study, a translocation line YNM158 with a YM158 genetic background and carrying the fragment of diploid *Th. elongatum* 7EL chromosome created by ^{60}Co-γ radiation showed high resistance to FHB under both filed and greenhouse conditions. The transcriptome analysis validated that the horizontal transfer gene *GST* is one of the important contributors to FHB resistance in pathogen infection stage, whereas 7EL chromosome fragment also carries other genes regulated by *F. graminearum* during the colonization stage. In addition, the introgression of 7EL fragment affected the expression of wheat genes which were enriched in the resistance pathways including phosphatidylinositol signaling system, protein processing in endoplasmic reticulum, plant-pathogen interaction and MAPK signaling pathway at different stages after *F. graminearium* infection.

Conclusions

The study provides a novel germplasm for wheat resistance to FHB and new insights into the molecular mechanism of wheat resistance to FHB.

Introduction

Fusarium head blight (FHB) is a primary disease caused by pathogens such as *F. asiaticum* and *F. graminearium*, seriously affecting yield and quality in wheat worldwide. Wheat infected with FHB, in addition to causing a significant reduction in yield, also accumulates the toxin deoxynivalenol (DON) in the seeds, which poses a significant risk to food safety. With global warming and changes in farming systems and practices, there is a trend of expanding the area of occurrence of the wheat blast, and the cultivation of blast-resistant varieties is the fundamental way to reduce its damage. However, the sources of resistance to wheat FHB were relatively narrow. There were only seven QTLs (*Fhb1*-*Fhb8*) related to FHB resistance, such as *Fhb1* from chromosome 3BS and *Fhb2* from chromosome 6BS of Sumai 3 [1, 2], *Fhb4* from chromosome 4B, *Fhb5* from chromosome 5A *Fhb8* from chromosome 7D of Wangshuibai [3–5], of which *Fhb1* was recognized as the most stable master effect QTL for FHB resistance expansion and widely used in wheat breeding for the FHB resistance. Furthermore, the QTLs were also found in wheat relatives, such as *Fhb3* from *Leymus racemosus* [6], *Fhb6* from *Elymus tsukushiensi* [7] and *Fhb7* from *Thinopyrum ponticum* [8, 9].

As an essential close relative of wheat, tall wheatgrass has many important favorable traits, which represent a valuable source of alien gene resources for wheat. Studies have shown that there are three species of tall wheatgrass in nature, namely *Th. elongatum* (diploid, 2n = 2x = 14, E^eE^e), *Th. scirpeum* (tetraploid, 2n = 4x = 28, $E^eE^eE^bE^b$) and *Th. ponticum* (decaploid, 2n = 10x = 70, $E^eE^eE^bE^bE^xE^x$StStStSt). There is no scientific conclusion on the evolution process of polyploidy of the family in *Thinopyrum*, but it is believed that many interspecific hybridizations and natural doubling of chromosomes occurred during the evolution process of tall wheatgrass which was similar to common wheat [10]. Because tall wheatgrass has strong resistance to wheat FHB, so far, breeders have constructed wheat-tall wheatgrass chromosome addition line, substitution line and other genetic materials by distant hybridization using *Th. elongatum* and *Th. ponticum*, and obtained the results related to FHB resistance. For example, Jauhar et al. created 1E addition lines, 1E (1A) and 1E (1B) diploid substitution lines by crossing durum wheat with diploid *Th. elongatum*, and found that the 1E chromosome of diploid *Th. elongatum* may carry FHB resistance genes by FHB resistance evaluation [11, 12]. Liu et al. (2017) obtained a disomic alien addition line with a pair of 7E *Th. scirpeum* chromosomes by hybridization of durum cultivar “Langdon” with the amphiploid 8801 (AABBEE) and found this addition lines showed high resistance to FHB [13]. Shen et al. identified the FHB resistance in the substitution lines 7E(7A), 7E(7B) and 7D(7E) from *Th. elongatum*, and $7el_2$ from *Th. ponticum* in the Thatcher genetic background [14]. This FHB resistant locus, assigned as *FhbLoP*, was mapped to the distal region of the long arm of chromosome 7E in *Th. ponticum* within a 3.71 cM interval flanked by *Xcfa2240* and *Xswes19*, which accounts for 30.46% of the phenotypic variance [15]. This locus was then designated as *Fhb7* and was fine mapped in 1.7 cM interval. Translocation lines with shortened *Th. ponticum* chromatin carrying *Fhb7* was developed [8]. After that, Wang et al. [9] successfully cloned the *Fhb7* gene from the *Th. ponticum* $7el_2$ chromosome by assembling the genome of *Th. elongatum*. And they proved that this gene encoded a glutathione S-transferase (GST), which can open the epoxy group of DON toxin and catalyze its formation of glutathione adduct (DON-GSH), resulting in detoxification and anti-FHB effect. However, Guo et al. discovered that some wheat-*Thinopyrum* derivatives carrying the *Fhb7* homologs had a different reaction to Fusarium head blight [16]. Similar results were also found in transgenic plants by overexpression of GST-encoding *Fhb7* [17].

Moreover, because *Th. elongatum, Th. scirpeum* and *Th. ponticum* shares the E genome of *Th. elongatum*, so previous studies have shown that the FHB resistance genes are also located on the homologous group seven in diploid *Th. elongatum* [13, 18]. For example, Zhang et al. incorporated a novel *Fhb7* allele, $Fhb7^{The2}$, into the wheat B genome through a small 7B-7E translocation (7BS·7BL-7EL) involving the terminal regions of the long arms, making this novel FHB resistance allele usable for breeding in both common and durum wheat [19].

It is well known that the introduction of chromosomes from wild species into wheat usually has linkage drag of undesirable genes and limits their application. In wheat genetic improvement, breeding translocation lines carrying alien beneficial genes, especially small fragment translocation lines, can reduce the linkage caused by alien chromosomes and has high genetic stability under common wheat

genetic background, which is an ideal way to introduce alien beneficial genes. Therefore, in this study, we aim to: obtain the translocation lines with different size of 7EL chromosome fragment; develop the stable inheritance translocation line with FHB resistance; evaluate the application value of translocation lines in wheat breeding for FHB resistance; explore potential disease resistance genes and analyze the disease resistance pathways in translocation lines through transcriptome analysis. The results can not only provide new germplasm for wheat FHB resistance breeding, but also provide a theoretical basis for studying the resistance mechanism of wheat FHB.

Result

Establishment of a wheat- Th. elongatum 7EL chromosome translocation line YNM158 with FHB resistance

When the alien chromosomes are introduced into wheat, there will be linkage drag, which will have a negative effect on the agronomic characters of wheat. So, creating the small segment translocation lines carrying the alien chromosomes can reduce the negative effects of linkage drag. In this study, the spikes of the translocation line T7BS·7EL, carrying the long arm of diploid *Th. elongatum* 7E chromosome, were treated by ^{60}Co-γ radiation during the flowering period of wheat. After treatment, the fresh pollen was collected and awarded to YM158 to obtain the M_1 seeds. The chromosomes of M_1 generation plants were identified by GISH, and the plants containing 7EL chromosome structure variation was selected for backcross with YM158. Finally, one line with stable agronomic characters was obtained in F_6 generation, which was named YNM158 (Fig. 1A). The root-tip cells of YNM158 at mitotic metaphase were analyzed by GISH and FISH. Firstly, the presence of the translocation chromosome pair was confirmed in YNM158 by GISH (Fig. 1B). Then, the chromosomal structural variation was observed on the end of 4BS chromosome according to the standard karyotype of CS (Fig. 1C). Finally, the translocation chromosome can be represented as T7EL4BS·4BL. In addition, the FHB resistance of YNM158 for two consecutive years showed that YNM158 has a high resistance to FHB in both field and greenhouse, and the level of FHB resistance was similar to that of SU3 (Fig. 1D and Table 1). Moreover, we observed almost no difference for the tested agronomic traits, including spike length, number of grains per spike, number of spikelets and grain width, for 2 consecutive years (Fig. 1E). However, plant height, thousand kernel, weight grain length and flag leaf area of YNM158 were significantly different compared with YM158 (Fig. 1E).

Table 1
Mean percentage of diseased spikelets (PDS) in different environments

Lines	2020–2021		2021–2022	
	Field	Greenhouse	Field	Greenhouse
YNM158	4.81% ± 0.19d	5.18% ± 0.37c	5.21% ± 0.23d	5.27% ± 0.20d
SU3	6.49% ± 1.79d	7.38% ± 2.89c	4.36% ± 0.22d	5.06% ± 0.21d
AN8455	83.42% ± 10.36a	75.83% ± 14.69a	87.88% ± 5.51a	60.19% ± 6.24a
YM23	28.79% ± 6.41c	53.69% ± 5.15b	15.54% ± 3.54c	21.87% ± 7.05c
YM158	47.01% ± 11.92b	-	31.80% ± 12.91b	45.09% ± 8.21b

Note: The data were statistically analyzed by Kruskal-Wallis one-way ANOVA. Pairwise comparisons were completed using LSD. Different letters show significance at $P < 0.05$.

RNA-seq data quality, assembly, and annotation of YNM158 and YM158

To analyze the genes associated with FHB resistance on chromosome 7EL chromosome segment in YNM158, RNA-sequencing (RNA-seq)-based transcriptome profiling was performed on the spikes which were inoculated F0609. In this experiment, total RNA was extracted from the spikes at 0-hours post-inoculation (hpi, no inoculation), 0.5 hpi, 2 hpi, 8 hpi, 24 hpi, 48 hpi, 72 hpi and 96 hpi, and 24 cDNA libraries were constructed (three repetitions per time). After filtering out the rRNAs and low-quality reads, a total of 193.57 GB high-quality clean data were obtained from 24 libraries (BioProject ID: PRJNA1011388), with an average of 80.65 GB clean data per library. The Q20 and Q30 were > 97% and > 93%, respectively. In addition, the GC contents were 48.86–52.53% among all samples. After assembly, the clean reads were mapped to the wheat and *Th. elongatum* reference genome (Chinese Spring v2.2 and *Th. elongatum* v1.0). On average, 91.17% of the reads were successfully aligned to the reference genome (Table S1). Therefore, these analyses indicated that the quality of our RNA-seq data was high and the sequencing depth was sufficient for further analysis.

To investigate the impact of chromosome translocations on gene expression, RNA-seq-based transcriptome profiling was also performed on wheat variety YM158 which was one of the parents of YNM158. In this study, we constructed cDNA libraries (24 cDNA libraries) of YM158 after *F. graminearum* infection at different time. After filtering out the rRNAs and low-quality reads, a total of 188.56 GB high-quality clean data were obtained from 24 libraries (BioProject ID: PRJNA1011388), with an average of 78.57 GB clean data per library. The Q20 and Q30 were > 97% and > 94%, respectively. After assembly, the clean reads were mapped to the wheat reference genome (Chinese Spring v2.2). On average, 89.31% of the reads were successfully aligned to the reference genome (Table S1). Therefore, these analyses indicated that the quality of our RNA-seq data was high and the sequencing depth was sufficient for further analysis.

Identification of the DEGs on 7EL chromosome post inoculation with F. graminearum

By using the criteria of FDR < 0.05, |log2 (fold change)| > 1, a total of 32102 differentially expressed genes (DEGs) were detected that significantly responses to *F. graminearum* infection at different times in YNM158, of which 222 DEGs were located on 7EL chromosome (Table S2). The 222 DEGs were analyzed, and the results showed that there were 60, 10, 25, 27, 49, 109 and 135 DEGs at 0.5 hpi, 2 hpi, 8 hpi, 24 hpi, 48 hpi, 72 hpi and 96 hpi, respectively (Fig. 2A). GO function enrichment analysis indicated that these DEGs were enriched in catalytic activity, carboxylic acid transmembrane transporter activity and organic acid transmembrane transporter activity in terms of molecular function. And a total of 124 DEGs were enriched in catalytic activity (Fig. 2B, Table S3). In terms of biological processes, organic anion transport, organonitrogen compound catabolic process and anion transport was the main role of the enriched genes. Among them, organonitrogen compound catabolic process was the term with the most enriched DEGs, with a total of 18 (Fig. 2B, Table S3). And the top 10 GO terms with the lowest Q value were selected to draw the scatter diagram of enrichment items in Fig. 2B. In addition, the KEGG pathway analysis revealed that the starch and sucrose metabolism pathway is the only one with the Q value less than 0.05 (Fig. 2C, Table S4). Moreover, the heatmap of the DEGs enriched in this pathway showed the expression levels of these genes were down-regulated after infection with *F. graminearum*, especially in the first 8 hours after infection (Fig. 2D). The top 10 pathways with the lowest Q value were selected to draw the scatter diagram of enrichment items in Fig. 2C.

Gene expression patterns analysis of DGEs on 7EL chromosome at different infection time-points

The trend analysis of 222 DEGs on 7EL chromosome showed that the DEGs were clustered into 20 profiles, of which 153 DEGs were significantly clustered to the three profiles, including profile 19, profile 0 and profile 6, on the basis of *P*-value 0.05 (Fig. 3A, Table S5). Among them, 77 genes showed a continuous upward trend with the extension of infection time (profile 19), and 56 genes showed a continuous downward trend (profile 0).

In addition, the 222 DEGs were analyzed of the weighted gene co-expression network analysis (WGCNA) modules associated with infection time. The selection of a soft threshold (Power) is the key step to constructing the network. When the soft threshold was set as 10 with a scale-free network fitting index of $R^2 > 0.80$, average connectivity was close to 0 (Fig. S1A). The hierarchical cluster tree was drawn based on the optimal soft threshold, and the genes clustered in the same branch are divided into the same module. Finally, four modules, including turquoise, blue, brown and grey, were obtained (Fig. S1B). Among them, the brown module was significantly correlated with infection at 0.5 hpi (R = 0.92, $P \leq 0.05$), the turquoise module was significantly correlated with infection at 8 hpi (R = 0.82, $P \leq 0.05$), and the blue module was significantly correlated with infection at 96 hpi (R = 0.69, $P \leq 0.05$). Based the cut-off criteria |module member-ship| (|MM|) > 0.8 and |gene significance| (|GS|) > 0.8, 19 genes with high connectivity in the clinically significant module were identified as hub genes (Fig. 3B and 3C, Table S6).

The DEGs and hub genes obtained from trend analysis and WGCNA, respectively, were sued to draw the Venn diagrams, and a total of 12 genes were obtained in both analyses (Fig. 3D, Table 2). The qRT-PCR verification of 12 DEGs showed that the relative expression levels of several genes were induced by *F. graminearium*, such as *Tel7E01G1020600*, *Tel7E01G943900* and *Tel7E01G980900*. Among them, *Tel7E01G1020600* encoded glutathione S-transferase (GST), whose expression was induced by *F. graminearium* and significantly upregulated from 72 hpi (Fig. 3E). *Tel7E01G943900* and *Tel7E01G1980900* had similar expression patterns, both of which were up-regulated at the early stage of infection. *Tel7E01G943900* encodes a receptor-like kinase, and the expression of this gene was up-regulated by about 5 times at 0.5 hpi, but then began to be down-regulated (Fig. 3F). Similarly, *Tel7E01G1980900* encoded a monosaccharide-sensing protein, the expression of this gene was significantly reached the highest level at 2 hpi, which was about 4 times than that at 0 hpi, but then began to be down-regulated and was almost no expression after 24 h of infection (Fig. 3G). These results suggested that there may be multiple resistance genes on chromosome 7EL fragment, which provide resistance to FHB at different stages of *F. graminearium* infection.

Table 2
The gene was verified by qRT-PCR.

Gene ID	Gene description
Tel7E01G1002700	Lysine ketoglutarate reductase trans-splicing-like protein (DUF707)
Tel7E01G1013700	Galactoside 2-alpha-L-fucosyltransferase
Tel7E01G1020600	Glutathione S-transferase
Tel7E01G211400	Protein kinase
Tel7E01G899900	NF-X1-type zinc finger protein NFXL1
Tel7E01G905000	Disease resistance protein (NBS-LRR class) family
Tel7E01G934300	Carbonic anhydrase
Tel7E01G939300	Receptor-like kinase
Tel7E01G941500	Carboxypeptidase
Tel7E01G943900	Receptor-like kinase
Tel7E01G946300	Blue copper binding protein
Tel7E01G980900	Monosaccharide-sensing protein 2

Extraction of wheat DEGs between YM158 and YNM158 after F. graminearum infection

Since wheat FHB is a compatible disease, Stephens et al., (2008) divided the infection process into initial colonization stage, infection stage and late infection stage [20]. In this study, we analyzed the effect of the introduction of 7EL chromosome fragments on FHB resistance using 8 hpi as the cut-off point. And we defined the initial colonization stage before 8hpi, the infection stage after 8hpi. First of all, 12761 and

15719 DEGs were obtained in the initial colonization stage and the infection stage, respectively (Table S7 and S8). Then, the DEGs at 0 hpi between YM158 and YNM158 were removed (Table S9). Finally, a total of 4734 DEGs were obtained at the initial stage of colonization (Fig. 4A), and 10489 DEGs were obtained at the stage of infection (Fig. 4B). After alignment with the reference genome, 4060 and 9808 wheat DEGs were screened for subsequent analysis at the initial colonization stage and infection stage, respectively (Fig. 4C, Table S10).

KEGG pathway enrichment analysis of wheat DEGs at different stages

To analyze the effect of 7EL chromosome on the resistance pathway of wheat at different stages after *F. graminearum* infection, the wheat DEGs were subjected to KEGG pathway enrichment analysis. We identified 7 pathways that were significantly enriched with a Q value less than 0.05 during the initial colonization stage, among which phosphatidylinositol signaling system was the most enriched pathway with the lowest Q value and the protein processing in endoplasmic reticulum pathway was the most enriched pathway with the DEGs number (Fig. 5A, Table S11). Further analysis of the genes involved in these pathways was found that the expression of some genes related to phosphatidylinositol 4-phosphate 5-kinase (PIP5K), immunoglobulin-binding protein (BIP4) and heat shock protein (Hsp) in YNM158 was higher than that in YM158 after *F. graminearum* infection (Fig. 5B).

At the infection stage, 21 specific pathways were significantly enriched with a Q value less than 0.05. Among them, glutathione metabolism was the pathway with the lowest Q value and the largest number of DEGs (Fig. 5C, Table S11). Moreover, genes related to ascorbate peroxidase (APX), glutathione reductase (GR), glutathione-S-transferase (GST) in this pathway were up-regulated in YNM158 (Fig. 5D). In addition, we also found that the genes related to ABC transporter (ATP-binding cassette, ABC) were up-regulated in YNM158, they may be associated with the transportation of DON (Fig. 5D). The plant-pathogen interaction pathway was the second most enriched pathway, with a total of 152 DEGs enriched in this pathway (Fig. 5C). Through the heat map of gene expression, we found that the expression levels of some genes related to hypersensitive response (HR), such as *TraesCS2D03G0030700* and *TraesCS2D03G1070500*, began to be up-regulated at 24 hpi with *F. graminearum* in YNM158 (Fig. 5D).

It is well known that secondary metabolites play an important role in plant resistance to pathogens. In our study, a total of 13 pathways were identified in both initial colonization stage and infection stages with a Q value less than 0.05. Among them, biosynthesis of secondary metabolites was the pathway with the lowest Q value (Fig. 5E and 5F, Table S12). The analysis of gene expression in this pathway found that some genes related to flavonol synthase (FLS), chalcone isomerase (CHI), chalcone synthase (CHS) and hydroxycinnamoyl-CoA shikimate (HCT) showed a significantly up-regulated expression trend with the extension of *F. graminearum* infection time in YNM158 (Fig. 5G). In addition, in the MAPK pathway, we also found the expression of some genes related to respiratory burst oxidase (RBOH) was significantly up-regulated after *F. graminearum* infection, and the expression level was the highest at 72 hpi, while the expression of some genes related to mitogen-activated protein kinase (MAPK) was up-

regulated at initial colonization stage and then down-regulated at the infection stage in YNM158 after *F. graminearum* infection in YNM158 (Fig. 5G).

WGCNA of wheat DEGs

The 12661 wheat DEGs were also analyzed of the WGCNA modules (Table S13). The selection of a soft threshold (Power) is the key step to constructing the network. When the soft threshold was set as 9 with a scale-free network fitting index of $R^2 > 0.80$, average connectivity was close to 0 (Fig. 6A and 6B). The hierarchical cluster tree was drawn based on the optimal soft threshold, and the genes clustered in the same branch are divided into the same module (Fig. 6C). Finally, 14 modules, which were correlated with varieties were obtained. Among them, the yellow module was significantly positive associated with YNM158 ($R = 0.96$, $P \leq 0.05$), and a total of 847 DEGs were obtained in this module (Fig. 6D, Table S14).

Screened the core genes at different infection stages

The Venn diagrams was drawn between the wheat DEGs at different infection stages and the hub genes positive associated with YNM158. At initial colonization stage, a total of 120 DEGs were obtained from the specific enrichment pathways (Table S15), and among them, 13 DEGs may be associated with the FHB resistance of YNM158 (Fig. 7A, Table S16). At infection stage, 830 DEGs were obtained from the specific pathway (Table S17), of which 10 DEGs may be related to the FHB resistance of YNM158 (Fig. 7B, Table S16). In addition, among the same pathways in both stages mentioned above, we obtained 202 DEGs (Fig. 7C, Table S18), 21 of which may be related the FHB resistance of YNM158 (Fig. 7D, Table S16).

In order to verify the correlation between the core genes and the stages of FHB resistance, these selected genes were verified by RT-PCR. Compared with the expression of YM158 at 0 hpi, we found that the expression levels of 6 wheat genes in YNM158 were significantly up-regulated after *F. graminearum* infection (Table 3). Among them, *TraesCS4D03G0528700* and *TraesCS4B03G0573000* belong to the phosphatidylinositol signaling system and protein processing in endoplasmic reticulum pathway, respectively. And had the same expression pattern at initial colonization stage, both of which were significantly up-regulated in YNM158. *TraesCS4D03G0528700* had the highest expression level at 2 hpi (Fig. 7E) and the expression of *TraesCS4B03G0573000* reached the highest level at 8 hpi (Fig. 7F). *TraesCS2D03G0030700* and *TraesCS7D03G0466200* encoded NBS-LRR disease resistance protein and 3-ketoacyl-CoA synthase, respectively, both belong to the plant-pathogen interaction pathway. However, their expression patterns were slightly different. The expression of *TraesCS2D03G0030700* was significantly up-regulated after *F. graminearum* infection and the expression of this gene in YNM158 was always higher than that of YM158 (Fig. 7G). Although *TraesCS7D03G0466200* was also induced after *F. graminearum* infection, the expression of *TraesCS7D03G0466200* in YNM158 was significantly higher than that in YM158 until 48 hpi (Fig. 7H). In addition, we found that the expression of one gene in biosynthesis of secondary metabolites and MAPK signaling pathway-plant was induced by *F. graminearum*. The results of RT-PCR indicated that these two genes may mediate the resistance of YNM158 to FHB during the initial colonization stage and infection stage. *TraesCS7A03G1308100*

encoded hydroxycinnamoyl-CoA shikimate, the expression of this gene in YNM158 was significantly higher than that in YM158 from 8 hours after *F. graminearum* infection (Fig. 7I). On the contrary, the expression of *TraesCS1A03G0718100* was significantly up-regulated at 0.5 hpi in YNM158. However, there was little difference in the expression of this gene between YM158 and YNM158 after 48 hpi (Fig. 7J). The above results suggest that the introduction of 7EL chromosome fragments may affect the disease resistance pathway of wheat, thereby improving the FHB resistance of wheat.

Table 3
The core genes verified by RT-PCR at different infection stages.

Gene ID	Pathway	Gene description
Initial colonization stage		
TraesCS4D03G0528700	Phosphatidylinositol signaling system	Phosphatidylinositol-4-phosphate 5-kinase family protein
TraesCS4B03G0573000	Protein processing in endoplasmic reticulum	70 kDa heat shock protein
Infection stage		
TraesCS2D03G0030700	Plant-pathogen interaction	NBS-LRR disease resistance protein
TraesCS7D03G0466200	Plant-pathogen interaction	3-ketoacyl-CoA synthase
Both stage		
TraesCS7A03G1308100	Biosynthesis of secondary metabolites	Hydroxycinnamoyl-CoA
TraesCS1A03G0718100	MAPK signaling pathway - plant	Respiratory burst oxidase-like protein

Discussion

YNM158 can be effectively applied in FHB improvement in wheat breeding

Breeding and applying FHB resistant varieties in wheat production is an effective way to control the destructive disease. However, the long-term intraspecific cross breeding of wheat reduced the range of genetic variation among varieties and had poor resistance to FHB, while the related wild species and genera of wheat carry many FHB resistance genes. For example, the FHB resistance genes *Fhb3*, *Fhb6* and *Fhb7* on chromosome 7Lr#1S of *Leymus racemosus*, chromosome 1E(ts)#1S of *Elymus tsukushiensis* and chromosome $7el_2$ of *Th. ponticum*, respectively were reported to have major resistance to FHB [6–9]. In addition, the $1Y^c$ and $3S^c$ chromosomes of *Roegneria ciliaris* [21], the 1E, 7E chromosome of diploid *Th. elongatum*, the chromosome 3St of *Elymus repens* [22], and the $7M^g$ chromosome of *Aegilops geniculata* [23] also possessed the FHB resistance genes. Although the

introduction of alien chromosomes can improve the resistance to FHB, it also brings some genetic encumbrance, which makes the agronomic characters of most foreign germplasm poor and difficultly to be directly used in wheat breeding for FHB resistance. Therefore, to make full use of wheat related species in wheat breeding for FHB resistance, it is necessary to create small fragment translocation lines to develop new varieties with increased FHB resistance and no yield penalty. At present, *Fhb7* gene from *Th. ponticum* was poured into cultivated wheat through small segment translocation lines and used in wheat breeding for FHB resistance [9]. The diploid form of tall wheatgrass, *Th. elongatum*, has a high level of resistance to FHB and was used to increase FHB resistance in wheat cultivar Chinese Spring by translocation development [19, 24]. In this study, we have successfully established the translocation lines with the small fragments of chromosome 7EL from diploid *Th. elongatum* by physical radiation, one of which has excellent agronomic traits and high resistance to wheat FHB and named YNM158. Different from previous reports, the translocation in YNM158 occurred on chromosome 4BS, a non-compensative translocation, and the reason for this phenomenon was that chromosome translocation was induced by ionizing radiation, the breakage and reconnection of wheat and alien chromosomes were random, so most of them were uncompensated translocations. Interestingly, the survey results of agronomic traits for two consecutive years showed that YNM158 did not have any bad performances due to a non-compensatory translocation line, such as genetic instability of exogenous chromosomes, high plant height and poor fertility. This may be because a small alien chromosome fragment was attached to the distal end of 4BS chromosome in recurrent parent in YNM158, whereas no chromosome fragments were lost in wheat. And previous studies have also shown that non-compensatory translocation lines also have important utility in wheat breeding. For example, the small fragment translocation line 5VS-6AS·6AL can be used to improve the quality of wheat soft grains [25], the 3A-7J^{S} translocation line can be used to improve wheat stem rust resistance [26], two homozygous translocation lines T1AS·1AL-6VS and T4BS·4BL-6VS-4BL carrying *Pm21* can be used to enhance powdery mildew resistance in wheat [27]. Therefore, we propose the translocation line YNM158, contained small fragment of 7EL chromosomes, has a good application prospect in the breeding for resistance to FHB in wheat.

Transcriptome analysis validated that glutathione metabolic is one of the important contributors to FHB resistance in pathogen infection stage

Transcriptome analysis is a valuable tool in investigating the molecular mechanisms behind cereal resistance to fungal infections as the costs of this technique decrease and its applications become more widespread. In this study, we found that compared with YM158, the glutathione metabolic was the most significantly enriched pathway in YNM158 after *F. graminearum* infection during the infection stage (Fig. 5D). It is well known that plants respond to fungal infections by activating defense genes including producing reactive oxygen species (ROS) which can enhance the strength of plant cell wall to resist the invasion and colonization of pathogens [28, 29]. However, when ROS accumulates in large amounts in plants, it will cause oxidative stress, damage plant cells, and lead to cell dysfunction and even death. Currently, the enzymes involved in the antioxidant defense system can be divided into two groups: (i) Enzymatic antioxidants such as superoxide dismutase (SOD), catalase (CAT), ascorbate peroxidase (APX), guaiacol peroxidase GPX, glutathione reductase (GR), monodehydroascorbate reductase

(MDHAR), and dehydroascorbate reductase (DHAR); (ii) Non-enzymatic antioxidants such as ascorbic acid (AA), reduced glutathione (GSH), α-tocopherol, carotenoids, plastoquinone/ubiquinone and flavonoids [30]. Early research reported that ascorbate-glutathione (AsA-GSH) cycle is the important way to diameter of removal of ROS in plant. Among them, APX is the key enzymes of this cycle, which can utilize AsA as the electron donor reducing H_2O_2 to water, and prevents the accumulation of a toxic level of H_2O_2 in photosynthetic organisms under stress conditions [31]. And the glutathione (GSH) participate in various metabolic processes and were the essential components of antioxidative and detoxification systems in plant cells [32]. It can be used as both a reducing agent and a strong nucleophile, participating in the elimination of reactive oxygen species (ROS) through thiol-disulphide redox reactions, and in the detoxification of various heterogenic organisms through conjugation reactions, respectively [33]. However, GSH will be oxidized to oxidized glutathione (GSSG) in the reaction of clearing ROS. In order to maintain the balance of GSH content in the plant, GR enzyme will effectively and timely reduce GSSG to GSH. It can be seen that GR enzyme plays a very important role in clearing ROS and maintaining the content of GSH in plants. For example, overexpression of *GR* gene from *Haynaldia villosa* in wheat can increase resistance to powdery mildew [34]. In this study, we found that the expression of some APX-encoding and GR-encoding genes in YNM158 was up-regulated during the infection stage (Fig. 5D). Therefore, we suggest that, glutathione may play a key role in ROS-mediated resistance to FHB in wheat.

In addition, glutathione S-transferase (GST) represents a group of multifunctional enzymes widely present in plants and plays important roles in plant secondary metabolism [35], growth and development [36], and biotic and abiotic stress responses [37]. Furthermore, one of its most important functions is the ability to inactivate toxic compounds. Because GST can form complexes with glutathione (GSH) by catalyzing hormones, toxins to inactivate or eliminate toxicity of many substances, and expel them in the body under the action of relevant transporters [38]. These results suggested that GST played a crucial role in plant disease resistance. For example, *NbGSTU1* can increase the resistance to *Colletotrichum destructivum* in *Nicotiana benthamiana* [39]. The lack of *GSTU13* function resulted in enhanced disease susceptibility toward several fungal pathogens in *Arabidopsis thaliana* [40]. Overexpression of *LrGST5* in tobacco can improve the resistance of transgenic plants to *F. oxysporum* [41]. *TaGSTU6* interactions can enhance wheat resistance to powdery mildew but not wheat stripe rust [42]. We know that wheat infected with FHB can be contaminated with a variety of mycotoxins, especially deoxynivalenol (DON) [43]. It has been reported that GSH can form a GSH-DON conjugates under the catalysis of GST to reduce the accumulation of DON and protect plants from toxicity. For instance, *Fhb7* and *FhbRc1*, encoding glutathione S-transferase, enhanced the resistance to FHB in wheat background [9, 44]. In this study, the expression of GST- encoding genes, including *TraesCS1A03G0109100*, *TraesCS3D03G0946300*, *TraesCS4D03G0493500*, *TraesCS5B03G0050700*, *TraesCS5A03G0730500*, *TraesCS5B03G0770700* and *Tel7E01G1020600* was significantly up-regulated after infection with *F. graminearum* in YNM158. Among them, the expression of the *Fhb7* homolog *Tel7E01G1020600* increased sharply at 72 hpi, which was tens of times higher than that of the non-infection (Fig. 3E). It can be seen that GST is one of the important contributors to FHB resistance roles in pathogen infection stage. However, the *Tel7E01G1020600* in YNM158 was derived from diploid *Th. elongatum*, which is not consistent with the

origin of Fhb7. So, whether *Tel7E01G1020600* in YNM158 has the same disease resistance function as *Fhb7* needs to be further studied.

Other genes from 7EL fragment in YNM158 might also be involved in increasing FHB resistance especially in pathogen initial colonization stage

DON toxin is a very important fungal pathogen when *F. graminearum* infects wheat. It can synthesize a large amount of *F. graminearum* along the inflorescence axis and promote the process of disease expansion. However, some studies have reported that when the pathogen initially infected wheat anthers, there was no DON synthesis signal, and only when the disease spread along the inflorescence axis from the inoculation point, DON began to be synthesized in large quantity in the pathogen [45, 46]. It can be seen that DON can help the pathogen spread along the wheat spike axis, but it is not necessary for its initial infection [47]. In the process of long-term co-evolution between plants and pathogens, a series of complex defense mechanisms have gradually formed. Generally, pathogen-associated molecular pattern (PAMP)-trigged immunity (PTI) is the first defensive line of plant innate immunity and is mediated by pattern recognition receptors (PRRs). And the PRRs are divided into two types, receptor-like kinases (PLKs) and receptor-like proteins (PLPs). To date, many PLKs have been found to play a key role in wheat disease resistance. For example, Sun et al. (2023) reported that a repeat receptor-like kinase-encoding gene *TaBIR1* contributed to wheat resistance against *Puccinia striiformis f. sp. tritici* by mediating ROS production and callose deposition [48], and the cysteine-rich receptor-like kinase TaCRK3 contributed to defense against *Rhizoctonia cerealis* in wheat through directing antifungal activity and heightening the expression of defense-associated genes in the ethylene signaling pathway [49]. And the RLKs have also been found to contribute to grain resistance to *Fusarium* resistance in cereals. For instance, Thapa et al. (2018) identified two homologous genes on barley chromosome 6H (HvLRRK-6H) and wheat chromosome 6DL (TaLRRK-6D), respectively, which could enhance cereal resistance to FHB disease [50]. And the Arabidopsis senses *Fusarium* elicitors in early immune responses to extracts from *Fusarium* spp. by a novel receptor complex which was encoded by the leucine-rich repeat receptor-like kinase MDIS1-interacting receptor-like kinase 2 (MIK2) at the cell surface [51]. Interesting, we also identified several RLKs-encoding genes on the 7EL fragment in this study, and the expression of them was significantly up-regulated at initial colonization stage after *F. graminearum* inoculation, such as the expression of *Tel7E01G943900* which was significantly up-regulated at 0.5 hpi (Fig. 3F).

In addition, in immune responses, plants have developed a number of disease-resistance mechanisms to resist nutrient uptake by pathogens, which involve sugar transport, metabolism, and signal transduction. The previous studies have shown that hexose released by cell wall invertase (CWIN) activity not only acts as a signal molecule to trigger the expression of disease-resistance related genes, but also is an essential metabolite and energy source for the synthesis of antioxidant compounds and defense molecules, such as salicylic acid and callose [52–54]. For example, *AtSTP4* and *Atβfruct1* encoding monosaccharide transporter and CWIN, respectively, are both induced in *Arabidopsis* during parasitic infection by fungus [55]. Chang et al. (2020) reported that silence the hexes transporter-encoding gene *PsHXT1* in wheat stripe rust can significantly inhibit the pathogenicity of pathogenic bacteria [56]. In this

study, the expression of a monosaccharide-sensing protein-encoding gene *Tel7E01G980900* was significantly up-regulated within 8h after infection with *F. graminearum* and reached the highest level at 2 hpi in YNM158 (Fig. 3G). And knowledge of the function of monosaccharide-sensing protein is similar to that of hexose transporters [57, 58]. Therefore, we speculated that they can also be conducted with CWINs to bring hexose back to host cells, reducing sugar availability to the pathogen, and thus improve host disease resistance. But this needs to be confirmed in the further studies.

It is well known that *F. graminearum* is a kind of facultative trophic bacteria. Therefore, wheat needs to use a series of defense mechanisms to resist pathogen infection at different stages. The introduction of 7EL chromosome fragments not only brought GST-encoding gene which was one of the important contributors on DON detoxification, but also brought other genes which were up-regulated at initial colonization stage. And these genes were also involved in increasing FHB resistance. Therefore, in-depth study of these genes can provide new insights into the molecular mechanisms of wheat resistance to FHB.

Introgression of 7EL fragment altered the gene expression in wheat after F. graminearum inoculation

The introduction of alien chromosome fragments not only brought the resistance genes, but also affects gene expression on normal chromosomes [59, 60]. In this study, we also found that the translocation of chromosomes affected the expression of wheat genes which were enriched in the resistance pathways including phosphatidylinositol signaling system, protein processing in endoplasmic reticulum, plant-pathogen interaction and MAPK signaling pathway at different stages with *F. graminearium* infection.

When plants are infected with pathogens, phospholipase C (PLC) is rapidly activated by different pathogen-associated molecular patterns (PAMPs) and effector proteins in plant cells [61]. And then catalyze phosphatidylinositol 4-phosphate (PI4P) and phosphatidylinositol (4,5) bisphosphate [PI(4,5)P2] to produce inositol 2-phosphate (IP2) or inositol 3-phosphate (IP3) and diacylglycerol (DAG). These are conserved compounds of pathogenic microbes that are perceived by immune receptors present in resistant plants [62, 63]. The previous studies reported that silencing and knock-out *SlPLC2* in tomato can reduce susceptibility to *Botrytis cinereal* [61, 62]. And the *SlPLC6* plays a key role in both for Ve1 resistance protein mediated resistance to *Verticillium dahliae* and Pto/Prf resistance protein mediated resistance to *Pseudomonas syringae* [64]. In addition, it has been reported that salicylic acid (SA), jasmonate (JA)and methyl jasmonate can increase the expression of *OsPI-PLC* in rice (*Oryza sativa*) and improve the resistance of rice to *Magnaporthe oryzae* [65]. In this study, it was found that the expression of some *PLC* genes in YNM158 was higher than that in YN158 at the initial colonization stage, such as *TraesCS4A03G0225500* and *TraesCS4B03G0547100*. Moreover, the results of qRT-PCR showed that the expression of *TraesCS4D03G0528700*, which encoded phosphatidylinositol 4-phosphate-5 kinase (PIPK5), in YNM158 was higher than that in YM158 at initial colonization stage (Fig. 7B). We know that PIP5K was the catalytic enzyme for the synthesis of PI(4,5)P2 and Shimada et al., (2019) have pointed out that the biosynthesis of PI(4,5)P2 was an important target to improve the defense ability of *Arabidopsis thaliana* against Colletotrichum, and its activity also determines the defense ability of

Arabidopsis thaliana against Colletotrichum [66]. Therefore, we speculated that PIP5K gene can affect the accumulation of PI(4,5)P2 in YNM1158 to participate in the PLC-mediated response to *F. graminearium* infection, and thus affect the colonization of *F. graminearium* to improve the resistance to FHB during the initial stages of infection.

There are also defense-related proteins in plants that are synthesized by the rough endoplasmic reticulum (RER), so when plants attacked by the pathogen, the genes encoding endoplasmic reticulum (ER) chaperones are induced, such as the immunoglobulin-binding protein (BIP), heat shock protein (Hsp), calreticulin (CRT) and protein disulfide isomerase (PDI)-encoding genes. The previous studies have shown that the Hsp was one of the ER chaperones, which play an indispensable role as molecular chaperones in the quality control of PRRs and intracellular resistance (R) proteins against potential invaders [67]. For example, Hsp90 was not only involved in the defense of many microbial pathogens by activating the cytosolic R proteins containing nucleotide-binding domain and a leucine-rich repeat, but also participated in chitin responses and anti-fungal immunity in a chaperone complex with its co-chaperone Hop/Sti1 [67, 68]. In terms of specific diseases, cytoplasmic *Capsicum annuum* Hsp70 (CaHsp70) can enhance the resistance to *Xanthomonas campestris* pv. *vesicatoria* in pepper [69], GmHsp40 can increase soybean resistance to Soybean *mosaic virus* [70], Hsp70 can enhance the resistance to powdery mildew in cucumber under heat shock-induction [71], MeHsp90.9-MeSGT1-MeRAR1 chaperone complex interacted with MeATGs to trigger autophagy signaling to improve disease resistance to cassava bacterial blight [72]. In this study, we found the expression of *TraesCS4B03G0573000*, which encodes the heat shock protein in YNM158 significantly induced to be upregulated after infection by *F. graminearium* at initial colonization stage, which was opposite to the expression pattern in YM158 (Fig. 7F). Usually, the expression of the genes encoding ER chaperones even predates the expression of genes encoding pathogenesis-related (PR) proteins [73]. Therefore, we inferred that the expression of genes encoding Hsp protein would rapidly induce after infection with *F. graminearium* in YNM158, thus activating the defense mechanism earlier, inducing programmed cell death, affecting the colonization of pathogens, and making plants resistant to disease, which provides a new idea for further research on the mechanism of FHB resistance.

Reactive oxygen species (ROS) are the important signaling molecules in defense responses during plant-pathogen interactions, which are mainly produced by respiratory burst oxidase homologs (RBOHs) [74]. In Arabidopsis, *AtRBOHD* and *AtRBOHF* are responsible for ROS production against pathogen attacks [75]. In *Nicotiana benthamiana*, *NbRBOHA* and *NbRBOHB* silencing leads to less ROS production and reduced the resistance against the infection by potato pathogen *Phytophthora infestans* [76]. Phosphorylation is known to be one of the essential mechanisms of RBOHD activation and is also transcriptionally activated by some kinases, such as MAPK cascades, and the transcriptional regulation of RBOHs may play a key roles in subsequent ROS bursts after turnover of the plasma membrane-localized RBOHs used for the first burst [77]. For example, Yamamizo et al. (2007) reported that MAPK kinase was involved in inducing the response of potato *StRBOHC* and *StRBOHD* genes in response to pathogen signals in potato [78], and Asai et al. (2008) also illustrated that the MAPK cascade MEK2-SIPK regulates the oxidative burst resulting from the induction of *RBOHB* expression in resistance to *P.*

infestans and *Colletotrichum orbiculare* of *N. benthamiana* [79]. Here, we identified the expression of a RBHO-encoded gene *TraesCS1A03G0718100* was up-regulated after *F. graminearum* infection in YNM158 (Fig. 7J), as well as some genes encoding MAPK kinase (Fig. 5G). Therefore, we hypothesized that MAPK kinase in YNM158 might be involved in inducing RBOH gene response to the resistance against *F. graminearum*. However, this puzzle requires further investigations.

Conclusions

FHB is a devastating wheat disease that seriously affects the yield and quality of wheat. Up to now, many laboratories around the world have carried out researches on wheat resistance to FHB. It has been proved by practice that the most economical and effective way to resist the damage of wheat FHB is to mine the genes with high resistance to FHB and breed new varieties resistant to FHB. In this study, a translocation line YNM158 carried 7EL chromosome fragment obtained by distant hybridization not only has excellent resistance to FHB, but also had stable agronomic traits that could potentially be used in FHB resistance breeding. Moreover, transcriptome analysis showed that the 7EL chromosome fragment not only carried the genes that can detoxify DON, but also have the genes that can affect the colonization of *F. graminearum* during the early stage of infection. In addition, the introgression of 7EL fragment altered the gene expression and activated the special resistance pathway in YNM158 after *F. graminearum* inoculation. It is demonstrated that YNM158 may have a variety of molecular mechanisms to against *F. graminearum* infection, and show a high resistance to FHB phenotype. Therefore, these results not only provide a new germplasm for wheat resistance to FHB, but also provide new insights into the molecular mechanism of wheat resistance to FHB, and also provide a new way for breeding new varieties with high resistance to FHB.

Materials and Methods

Plant materials

Triticum aestivum cv. Chinese Spring (CS), Su Mai3 (SU3), An Nong8455 (AN8455), and Yang Mai158 (YM158) are maintained at Yangzhou University, China. Wheat cultivar YM158 was pollinated with the ^{60}Co-γ-irradiated pollen of the long-arm translocation line TW-7EL1 (T7BS·7EL) of 7E chromosome with excellent FHB resistance developed in previous studies. The small fragment of 7EL chromosome translocation line Yangnongmai158 (YNM158) was selected from the hybrid progeny in this study.

Cell cycle synchronization and preparation of mitotic chromosomes

Cell cycle synchronization and slide preparation followed Lei et al. [80] with minor modifications. Seeds were soaked in water for 3–5 hours and germinated on moist filter paper for 2 days in the dark at 25°C. When the roots grew to about 2.5 cm long, the roots were treated with 2 μmol/L amiprophosmethyl (APM) for 2.5 h. Then the root tips were cut off and treated in a nitrous oxide gas chamber for 1 h. After

that the root tips were fixed in ice-cold 90% acetic acid for 8 min, washed with sterile distilled water (ddH_2O) and stored in 70% ethanol at -20°C until use. For slide preparation, root tips were washed in ddH_2O for 5 min. The apical meristem of roots was cut and incubated in 25 μL of enzyme solution containing 2% cellulase Onozuka R-10 (Yakult Pharmaceutical, Tokyo) and 1% pectolyase Y23 (ICN) for 1 h at 37°C in a water bath. Meristems were separated with a needle in 50 μL of 100% acetic acid and immediately dropped onto microscope slides using a pipette at a height of approximately 10 cm and then placed in a wet box for about 20 min. The number and location of chromosomes were observed and recorded under the phase contrast objective (Nikon 80i, Japan), and the well-prepared slides were stored in a -70°C refrigerator until use.

Genomic in situ hybridization (GISH) and Fluorescence in situ hybridization (FISH) analysis

The techniques of GISH and ND-FISH followed those of Tang et al. [81]. Total genomic DNA of *Th. elongatum* was labeled with digoxigenin-12-dUTP by Nick Translation method and used as a probe for GISH. The repetitive sequences oligo-pSc119.2 and oligo-pAs1 were synthesized as the probes. And the 5’ end of oligo-pSc119.2 was labeled by 6-carboxyfluorescein (6-FAM), the 5’ ends of oligo-pAs1 was labeled by 6-carboxytetramethylrhodamine (Tamra). The labeled probes were dissolved in 2 × SSC and 1× TE buffer (pH 7.0), dropped to the prepared slides. After that the slides were covered with a coverslip and placed in a humidified hybridization cassette at 37°C for 10 h, and then transferred into 2×SSC for 2 min at room temperature. Finally, the slides were quickly dried, and then 6.5 μL DAPI was added to each slide (Vector, No. H-1200). After ND-FISH analysis, the slides were washed in 2×SSC for 2 min at room temperature. After drying the same slides were subjected to GISH analysis. Hybridization signals were observed using a fluorescent microscope and images were obtained with a CCD camera (Color Cooled Digital DS-Fi1c, Nikon 80i, Japan).

Evaluation of Disease Resistance

The translocation line YNM158 and its hybrid offspring were screened for FHB resistance in the field and greenhouse in 2021 and 2022. At early flowering stage, the central spikelet was injected into 10 μL fungal suspension (50,000 spores/mL), and at least three spikes from each plant was injected. Following inoculation, the plants were misted for 72 h for FHB development. After 21 days, all infected spikelets per inoculated spike were counted. Wheat cultivars An8455 served as the susceptible controls in both the field and greenhouse, respectively, and SU3 served as the resistant control in both the field and greenhouse.

De novo assembly of RNA-seq reads and quantifying gene expression

The transcriptome analysis was comprised of 8 time points after inoculation with *F. graminearum*: 0 hpi, 0.5 hpi, 2 hpi, 8 hpi, 24 hpi, 48 hpi, 72 hpi and 96 hpi. Three spikes after inoculation was randomly selected for each time were mixed to extract RNA. Total RNA was extracted using Trizol reagent kit

(Invitrogen) according to the manufacturer's protocol. RNA quality was assessed on an Agilent 2100 Bioanalyzer (Agilent Technologies) and checked by using RNase-free agarose gel electrophoresis. The mRNA was enriched by Oligo (dT) beads. Then the enriched mRNA was fragmented and used as the template for cDNA synthesis. The cDNA fragments were sequenced using Illumina HiSeq2500 by Gene Denovo Biotechnology Co. For the analysis process after sequencing, referred to the article published by Dai et al. [82]. The genome of Chinese Spring (IWGSC RefSeq v2.1) and the genome of *Th. elongatum* (GWHABKY00000000) were used as the reference genome in this study. The obtained sequences were submitted on the sequence read archive data (BioProject ID: PRJNA1011388).

Quantitative real-time polymerase chain reaction

Three spikes after inoculation was randomly selected for each time were mixed to extract RNA. qRT-PCR was performed under the following program: 94°C for 5 min, and then 40 cycles: 94°C for 5 min followed by 60°C for 30 s. For the melt curve analysis, the following program was included after 40 cycles: 95°C for 10 s followed by 60°C for 30 s and a constant increase from 60 to 95°C. The relative expression levels were determined using the $2^{-\Delta\Delta Ct}$ method. qRT-PCR assays were carried out in three independent biological samples pretreatment and three technical replicates per samples. The primers used for this analysis were shown in Table S19.

Data analysis

All data were statistically analyzed using the IBM SPSS Statistics 25 software with pairwise comparisons of LSD to identify differences. The data conforming to normal distribution and homogeneity of variance use one-way ANOVA; otherwise Kruskal-Wallis one-way ANOVA was used. Significant differences ($P < 0.05$) were indicated by different letters. The GraphPad Prism 8 software was used to draw figures.

Abbreviations

FHB	*Fusarium* head blight
DON	Deoxynivalenol
GST	Glutathione S-transferase
GSH	Glutathione
APM	Amiprophosmethyl
GISH	Genomic in situ hybridization
FISH	Fluorescence in situ hybridization
ND-FISH	Non-denaruring fluorescence in situ hybridization
hpi	Hours post-inoculation
DEG	Differentially expressed genes
PIP5K	Phosphatidylinositol 4-phosphate 5-kinase
BIP	Immunoglobulin-binding protein
Hsp	Heat shock protein
APX	Ascorbate peroxidase
GR	Glutathione reductase
HR	Hypersensitive response
FLS	Flavonol synthase
CHI	Chalcone isomerase
CHS	Chalcone synthase
HCT	Hydroxycinnamoyl-coa shikimate
MAPK	Mitogen-activated protein kinase
RBOH	Respiratory burst oxidase
WGCNA	Weighted gene co-expression network analysis
PTI	Pathogen-associated molecular pattern-trigged immunity
PRRs	Pattern recognition receptors
PLKs	Receptor-like kinases
PLPs	Receptor-like proteins
ROS	Reactive oxygen species
MIK2	MDIS-interacting receptor-like kinase 2

CWIN	Cell wall invertase
PLC	Phospholipase C
SA	Salicylic acid
JA	Jasmonate
RER	Rough endoplasmic reticulum
CRT	Calreticulin
PDI	Protein disulfide isomerase
PCR	Polymerase chain reaction

Declarations

Acknowledgments

We thank the participants for partaking in this study. The authors would like to thank the reviewers whose constructive comments are very helpful for strengthening the presentation of this paper.

Authors' contributions

Y.D., data curation, data analysis, visualization, methodology, writing-original draft. W.F., data analysis, material identification. S.C., data curation, investigation of agronomic traits, material planting. J.S., data analysis, material identification, evaluation of fhb resistance. H.L., material planting, material identification. J.L., investigation of agronomic traits, evaluation of FHB resistance. H.M. (Haigang Ma), evaluation of FHB resistance. Y.W., formal analysis, validation. Y.G., visualization. J.Z., and B.W., material radiation. J.C, conceptualization, supervision, data curation. H.M. (Hongxiang Ma), conceptualization, supervision, data curation, funding acquisition, project administration, resources, writing-review & editing.

Funding

This research was funded by the Project of Zhongshan Biological Breeding (ZSBBL-KY2023-02-3, BM2022008-02), Seed Industry Revitalization Project of Jiangsu Province (JBGS2021047), Jiangsu Key Project for the Research and Development (BE2022346), and a Project Funded by the Priority Academic Program Development of Jiangsu Higher Education Institutions (PAPD).

Availability of data and materials

The genome sequences of Chinese Spring were downloaded from the website: http://www.wheatgenome.org/News2/IWGSC-RefSeq-v2.0-now-available-at-URGI. The genome sequences of *Th. elongatum* were downloaded from the website: https://ngdc.cncb.ac.cn/gwh/Assembly/965/show. The transcriptome sequencing data generated in this study have been deposited in the NCBI Sequence Read Archive (SRA) database under accession number

PRJNA1011388. And the datasets generated or analyzed during this study are included in this article and its additional file or are available from the corresponding author on reasonable request.

Ethics approval and consent to participate

Not applicable.

Consent for publication

Not applicable.

Competing interests

The authors declare that they have no competing interests.

References

1. Cuthbert PA, Somers DJ, Thomas J, Cloutier S, Brule-Babel A. Fine mapping *Fhb1*, a major gene controlling *Fusarium* head blight resistance in bread wheat (*Triticum aestivum* L.). Theor Appl Genet. 2006;112:1465-1472.
2. Cuthbert PA, Somers DJ, Brule-Babel A. Mapping of *Fhb2* on chromosome 6BS: a gene controlling *Fusarium* head blight field resistance in bread wheat (*Triticum aestivum* L.). Theor Appl Genet, 2007;114:429-437.
3. Xue S, Li GQ, Jia HY, Xu F, Lin F, Tang MZ, Wang Y, An X, Xu HB, Zhang LX et al. Fine mapping *Fhb4*, a major QTL conditioning resistance to *Fusarium* infection in bread wheat (*Triticum aestivum* L.). Theor Appl Genet. 2010;121:147-156.
4. Xue SL, Xu F, Tang MZ, Zhou Y, Li GQ, An X, Lin F, Xu HB, Jia HY, Zhang LX et al. Precise mapping *Fhb5*, a major QTL conditioning resistance to *Fusarium* infection in bread wheat (*Triticum aestivum* L.). Theor Appl Genet. 2011;123:1055-1063.
5. Wang X, Li GQ, Jia HY, Cheng R, Zhong JK, Shi JX, Chen RT, Wen YX, Ma ZQ. Breeding evaluation and precise mapping of *Fhb8* for *Fusarium* head blight resistance in wheat (*Triticum aestivum*). Plant Breeding. 2023;143:26-33.
6. Qi LL, Pumphrey MO, Friebe B, Chen PD, Gill BS. Molecular cytogenetic characterization of alien introgressions with gene *Fhb3* for resistance to *Fusarium* head blight disease of wheat. Theor Appl Genet. 2008;117:1155-1166.
7. Cainong JC, Bockus WW, Feng YG, Chen PD, Qi LL, Sehgal SK, Danilova TV, Koo DH, Friebe B, Gill BS. Chromosome engineering, mapping, and transferring of resistance to *Fusarium* head blight disease from *Elymus tsukushiensis* into wheat. Theor Appl Genet. 2015;128:1019-1027.
8. Guo J, Zhang XL, Hou YL, Cai JJ, Shen XR, Zhou TT, Xu HH, Ohm HW, Wang HW, Li AF et al. High-density mapping of the major FHB resistance gene *Fhb7* derived from *Thinopyrum ponticum* and its pyramiding with *Fhb1* by marker-assisted selection. Theor Appl Genet. 2015;128:2301-2316.

9. Wang HW, Sun SL, Ge WY, Zhao LF, Hou BQ, Wang K, Lyu ZF, Chen LY, Xu SS, Guo J et al. Horizontal gene transfer of *Fhb7* from fungus underlies *Fusarium* head blight resistance in wheat. Science. 2020;368:eaba5435.
10. Dai Y, Huang S, Sun G, Li H, Chen J. Origins and chromosome differentiation of *Thinopyrum elongatum* revealed by *PepC*, *Pgk1* genes and ND-FISH. Genome. 2021;64:901-913.
11. Jauhar PP, Peterson TS, Xu SS. Cytogenetic and molecular characterization of a durum alien disomic addition line with enhanced tolerance to *Fusarium* head blight. Genome. 2009;52:467-483.
12. Jauhar, Prem P. Durum wheat genetic stocks involving chromosome 1E of diploid wheatgrass: resistance to Fusarium head blight. Nucleus. 2014;57:19-23.
13. Liu HP, Dai Y, Chi D, Huang S, Li HF, Duan YM, Cao WG, Gao Y, Fedak G, Chen JM. Production and molecular cytogenetic characterization of a durum Wheat-*Thinopyrum elongatum* 7E disomic addition line with resistance to *Fusarium* head blight. Cytogenet Genome Res. 2017;153:165-173.
14. Shen R, Kong LR, Ohm H. *Fusarium* head blight resistance in hexaploid wheat (*Triticum aestivum*)-*Lophopyrum* genetic lines and tagging of the alien chromatin by PCR markers. Theor Appl Genet. 2004;108:808-813.
15. Zhang XL, Shen XR, Hao YF, Cai JJ, Ohm HW, Kong LR. A genetic map of *Lophopyrum ponticum* chromosome 7E, harboring resistance genes to *Fusarium* head blight and leaf rust. Theor Appl Genet. 2011;122:263-270.
16. Guo XR, Wang M, Kang HY, Zhou YH, Han FP. Distribution, polymorphism and function characteristics of the GST-encoding *Fhb7* in *Triticeae*. Plants-Basel 2022, 11(16).
17. Guo XR, Shi QH, Wang M, Yuan J, Zhang J, Wang J, Liu Y, Su HD, Wang Z, Li JB et al. Functional analysis of the glutathione S-transferases from *Thinopyrum* and its derivatives on wheat *Fusarium* head blight resistance. Plant Biotechnol J. 2023;21:1091-1093.
18. Shen X, Ohm H. *Fusarium* head blight resistance derived from *Lophopyrum elongatum* chromosome 7E and its augmentation with *Fhb1* in wheat. Plant Breeding. 2006;125:424-429.
19. Zhang W, Danilova T, Zhang MY, Ren SF, Zhu XW, Zhang QJ, Zhong SB, Dykes L, Fiedler J, Xu S et al. Cytogenetic and genomic characterization of a novel tall wheatgrass-derived *Fhb7* allele integrated into wheat B genome. Theor Appl Genet. 2022;135:4409-4419.
20. Stephens AE, Gardiner DM, White RG, Munn AL, Manners JM. Phases of infection and gene expression of Fusarium graminearum during crown rot disease of wheat. Mol Plant Microbe In. 2008;21:1571-1581.
21. Kong LN, Song XY, Xiao J, Sun HJ, Dai KL, Lan CX, Singh PW, Yuan CX, Zhang SZ, Singh R et al. Development and characterization of a complete set of *Triticum aestivum-Roegneria ciliaris* disomic addition lines. Theor Appl Genet. 2018;131:1793-1806.
22. Gong BR, Zhu W, Li SY, Wang YQ, Xu LL, Wang Y, Zeng J, Fan X, Sha LN, Zhang HQ et al. Molecular cytogenetic characterization of wheat-*Elymus repens* chromosomal translocation lines with resistance to *Fusarium* head blight and stripe rust. BMC Plant Biol. 2019;19:590.

23. Yang XY, Xu MR, Wang YF, Cheng XF, Huang CX, Zhang H, Li TD, Wang CY, Chen CH, Wang YJ et al. Development and molecular cytogenetic identification of two wheat-*Aegilops geniculata* Roth $7M^g$ chromosome substitution lines with resistance to *Fusarium* head blight, powdery mildew and stripe rust. Int J Mol Sci. 2022;23(13):15.
24. Haldar A, Tekieh F, Balcerzak M, Wolfe D, Lim D, Joustra K, Konkin D, Han FP, Fedak G, Ouellet T. Introgression of *Thinopyrum elongatum* DNA fragments carrying resistance to *Fusarium* head blight into *Triticum aestivum* cultivar Chinese Spring is associated with alteration of gene expression. Genome. 2021;64:1009-1020.
25. Zhang RQ, Wang XE, Chen PD. Molecular and cytogenetic characterization of a small alien-segment translocation line carrying the softness genes of *Haynaldia villosa*. Genome. 2012;55:639-646.
26. Li J, Bao Y, Han R, Wang X, Xu W, Li G, Yang Z, Zhang X, Li X, Liu A et al. Molecular and cytogenetic identification of stem rust resistant wheat-*Thinopyrum intermedium* introgression lines. Plant Dis. 2022;106:2447-2454.
27. Chen PD, You CF, Hu Y, Chen SW, Zhou B, Cao AZ, Wang X. Radiation-induced translocations with reduced *Haynaldia villosa* chromatin at the *Pm21* locus for powdery mildew resistance in wheat. Mol Breeding. 2013;31:477-484.
28. Yang C, Liu R, Pang J, Ren B, Zhou H, Wang G, Wang E, Liu J. Poaceae-specific cell wall-derived oligosaccharides activate plant immunity via OsCERK1 during *Magnaporthe oryzae* infection in rice. Nat commu. 2021;12:2178.
29. O'Brien JA, Daudi A, Butt VS, Bolwell GP. Reactive oxygen species and their role in plant defence and cell wall metabolism. Planta. 2012;236:765-779.
30. García-Caparrós P, De Filippis L, Gul A, Hasanuzzaman M, Ozturk M, Altay V, Lao MT. Oxidative stress and antioxidant metabolism under adverse environmental conditions: a review. Bot Rev. 2021;87:421-466.
31. Pang CH, Wang BS. Role of ascorbate peroxidase and glutathione reductase in ascorbate-glutathione cycle and stress tolerance in plants. In: Anjum NA, Chan MT, Umar S, editors. Ascorbate-glutathione pathway and stress tolerance in plants. Dordrecht: Springer; 2010. p. 91-113.
32. Lu CC, Jiang YK, Yue YZ, Sui YR, Hao MX, Kang XJ, Wang QB, Chen DY, Liu BY, Yin ZY et al. Glutathione and neodiosmin feedback sustain plant immunity. J Exp Bot. 2023;74:976-990.
33. Gullner G, Kömives T. The role of glutathione and glutathione-related enzymes in plant-pathogen interactions. In: Grill D, Tausz M, Kok LJ, editors. Significance of glutathione to plant adaptation to the environment. Dordrecht, Springer; 2001. p. 207-239.
34. Chen YP, Xing LP, Wu GJ, Wang HZ, Wang XE, Cao AZ, Chen PD. Plastidial glutathione reductase from *Haynaldia villosa* is an enhancer of powdery mildew resistance in wheat (*Triticum aestivum*). Plant Cell Physiol. 2007;48:1702-1712.
35. Mueller LA, Goodman CD, Silady RA, Walbot V. AN9, a petunia glutathione S-transferase required for anthocyanin sequestration, is a flavonoid-binding protein. Plant Physiol. 2000;123:1561-1570.

36. Gong HB, Jiao YX, Hu WW, Pua EC. Expression of glutathione-S-transferase and its role in plant growth and development in vivo and shoot morphogenesis in vitro. Plant Mol Biol. 2005;57:53-66.
37. Ma LG, Zhang YH, Meng QL, Shi FM, Liu J, Li YC. Molecular cloning, identification of GSTs family in sunflower and their regulatory roles in biotic and abiotic stress. World J Microb Biot. 2018, 34:109.
38. Edwards R, Dixon DP, Walbot V. Plant glutathione S-transferases: enzymes with multiple functions in sickness and in health. Trends Plant Sci. 2000;5:193-198.
39. Dean JD, Goodwin PH, Hsiang T. Induction of glutathione S-transferase genes of Nicotiana benthamiana following infection by Colletotrichum destructivum and C. orbiculare and involvement of one in resistance. J Exp Bot. 2005;56:1525-1533.
40. Pislewska-Bednarek M, Nakano RT, Hiruma K, Pastorczyk M, Sanchez-Vallet A, Singkaravanit-Ogawa S, Ciesiolka D, Takano Y, Molina A, Schulze-Lefert P et al. Glutathione transferase U13 functions in pathogen-triggered glucosinolate metabolism. Plant Physiol. 2018;176:538-551.
41. Han Q, Chen R, Yang Y, Cui XM, Ge F, Chen CY, Liu DQ. A glutathione S-transferase gene from *Lilium regale* Wilson confers transgenic tobacco resistance to *Fusarium oxysporum*. Scientia Horticulturae 2016, 198:370-378.
42. Wang Q, Guo J, Jin PF, Guo MY, Guo J, Cheng P, Li Q, Wang BT. Glutathione S-transferase interactions enhance wheat resistance to powdery mildew but not wheat stripe rust. Plant Physiol. 2022;190:1418-1439.
43. Chen Y, Kistler HC, Ma ZH. *Fusarium graminearum* trichothecene mycotoxins: biosynthesis, regulation, and management. Annu Rev Phytopathol. 2019; 57:15-39.
44. Song RR, Cheng YF, Wen MX, Song XY, Wang T, Xia MS, Sun HJ, Cheng MH, Cui HM, Yuan CX et al. Transferring a new *Fusarium* head blight resistance locus *FhbRc1* from *Roegneria ciliaris* into wheat by developing alien translocation lines. Theor Appl Genet. 2023;136:36.
45. Ilgen P, Hadeler B, Maier FJ, Schäfer W. Developing kernel and rachis node induce the trichothecene pathway of *Fusarium graminearum* during wheat head infection. Mol Plant Microbe Interact. 2009;22:899-908.
46. Boenisch MJ, Schäfer W. *Fusarium graminearum* forms mycotoxin producing infection structures on wheat. BMC Plant Biol. 2011;11:110.
47. Mudge AM, Dill-Macky R, Dong YH, Gardiner DM, White RG, Manners JM. A role for the mycotoxin deoxynivalenol in stem colonisation during crown rot disease of wheat caused by *Fusarium graminearum* and *Fusarium pseudograminearum*. Physiol Mol Plant P. 2006;69:73-85.
48. Sun YC, Wang XJ, Liu FY, Guo HY, Wang JF, Wei ZT, Kang ZS, Tang CL. A leucine-rich repeat receptor-like kinase TaBIR1 contributes to wheat resistance against *Puccinia striiformis* f. sp. *tritici*. Int J Mol Sci. 2023;24:6438.
49. Guo FL, Wu TC, Shen FD, Xu GBA, Qi HJ, Zhang ZY. The cysteine-rich receptor-like kinase TaCRK3 contributes to defense against *Rhizoctonia cerealis* in wheat. J Exp Bot. 2021;72:6904-6919.
50. Thapa G, Gunupuru LR, Hehir JG, Kahla A, Mullins E, Doohan FM. A pathogen-responsive leucine rich receptor like kinase contributes to *Fusarium* resistance in cereals. Front Plant Sci. 2018;9:867.

51. Coleman AD, Maroschek J, Raasch L, Takken FLW, Ranf S, Hückelhoven R. The Arabidopsis leucine-rich repeat receptor-like kinase MIK2 is a crucial component of early immune responses to a fungal-derived elicitor. New Phytol. 2021;229:3453-3466.
52. Ruan YL. Sucrose Metabolism: gateway to diverse carbon use and sugar signaling. In: Annu Rev Plant Biol. 2014;65:33-67.
53. Liu YH, Offler CE, Ruan YL. Regulation of fruit and seed response to heat and drought by sugars as nutrients and signals. Front Plant Sci. 2013;4:282.
54. Xiang L, Le Roy K, Bolouri-Moghaddam MR, Vanhaecke M, Lammens W, Rolland F, Van den Ende W. Exploring the neutral invertase-oxidative stress defence connection in Arabidopsis thaliana. J Exp Bot. 2011;62:3849-3862.
55. Fotopoulos V, Gilbert MJ, Pittman JK, Marvier AC, Buchanan AJ, Sauer N, Hall JL, Williams LE. The monosaccharide transporter gene, AtSTP4, and the cell-wall invertase, At beta fruct1, are induced in Arabidopsis during infection with the fungal biotroph Erysiphe cichoracearum. Plant Physiol. 2003;132:821-829.
56. Chang Q, Lin XH, Yao MH, Liu P, Guo J, Huang LL, Voegele RT, Kang ZS, Liu J. Hexose transporter PsHXT1-mediated sugar uptake is required for pathogenicity of wheat stripe rust. Plant Biotechnol J. 2020;18:2367-2369.
57. Chen LQ, Qu XQ, Hou BH, Sosso D, Osorio S, Fernie AR, Frommer WB. Sucrose efflux mediated by SWEET proteins as a key step for phloem transport. Science. 2012, 335:207-211.
58. Sutton PN, Gilbert MJ, Williams LE, Hall JL. Powdery mildew infection of wheat leaves changes host solute transport and invertase activity. Physiologia Plantarum. 2010;129:787-795.
59. Harewood L, Fraser P. The impact of chromosomal rearrangements on regulation of gene expression. Hum Mol Genet. 2014;23:R76-R82.
60. Spielmann M, Lupianez DG, Mundlos S. Structural variation in the 3D genome. Nat Rev Genet. 2018;19:453-467.
61. Perk EA, Di Palma AA, Colman S, Mariani O, Cerrudo I, D'Ambrosio JM, Robuschi L, Pombo MA, Rosli HG, Villareal F et al. CRISPR/Cas9-mediated phospholipase C 2 knock-out tomato plants are more resistant to *Botrytis cinerea*. Planta. 2023;257:117.
62. Gonorazky G, Guzzo MC, Abd-El-Haliem AM, Joosten M, Laxalt AM. Silencing of the tomato phosphatidylinositol-phospholipase C2 (SlPLC2) reduces plant susceptibility to *Botrytis cinerea*. Mol Plant Pathol. 2016;17:1354-1363.
63. Laxalt AM, Munnik T. Phospholipid signalling in plant defence. Curr Opin Plant Biol. 2002;5:332-338.
64. Vossen JH, Abd-El-Haliem A, Fradin EF, van den Berg GCM, Ekengren SK, Meijer HJG, Seifi A, Bai YL, ten Have A, Munnik T et al. Identification of tomato phosphatidylinositol-specific phospholipase-C (PI-PLC) family members and the role of PLC4 and PLC6 in HR and disease resistance. Plant J. 2010;62:224-239.
65. Song FM, Goodman RM. Molecular cloning and characterization of a rice phosphoinositide-specific phospholipase C gene, OsPI-PLC1, that is activated in systemic acquired resistance. Physiol Mol

Plant P. 2002;61:31-40.

66. Shimada TL, Betsuyaku S, Inada N, Ebine K, Fujimoto M, Uemura T, Takano Y, Fukuda H, Nakano A, Ueda T. Enrichment of phosphatidylinositol 4,5-bisphosphate in the extra-invasive hyphal membrane promotes colletotrichum infection of Arabidopsis thaliana. Plant Cell Physiol. 2019;60:1514-1524.
67. Park CJ, Seo YS. Heat shock proteins: a review of the molecular chaperones for plant immunity. Plant Pathol J. 2015;31:323-333.
68. Chen LT, Hamada S, Fujiwara M, Zhu TH, Thao NP, Wong HL, Krishna P, Ueda T, Kaku H, Shibuya N et al. The Hop/Sti1-Hsp90 chaperone complex facilitates the maturation and transport of a PAMP Receptor in rice innate immunity. Cell Host Microbe. 2010;7:185-196.
69. Kim NH, Hwang BK. Pepper heat shock protein 70a interacts with the type III effector AvrBsT and triggers plant cell death and immunity. Plant Physiol. 2015;167:307-322.
70. Liu JZ, Whitham SA. Overexpression of a soybean nuclear localized typeIII DnaJ domain-containing HSP40 reveals its roles in cell death and disease resistance. Plant J. 2013;74:110-121.
71. Widiastuti A, Arofatullah NA, Kharisma AD, Sato T. Upregulation of heat shock transcription factors, Hsp70, and defense-related genes in heat shock-induced resistance against powdery mildew in cucumber. Physiol Mol Plant P. 2021;116: 101730.
72. Wei YX, Zeng HQ, Liu W, Cheng X, Zhu BB, Guo JR, Shi HT. Autophagy-related genes serve as heat shock protein 90 co-chaperones in disease resistance against cassava bacterial blight. Plant J. 2021;107:925-937.
73. Jelitto-Van Dooren E, Vidal S, Denecke J. Anticipating endoplasmic reticulum stress: A novel early response before pathogenesis-related gene induction. Plant Cell. 1999;11:1935-1943.
74. Wu B, Qi F, Liang Y. Fuels for ROS signaling in plant immunity. Trends in plant science. 2023; 28:1124-1131.
75. Torres MA, Dangl JL, Jones JDG. *Arabidopsis* gp91^{phox} homologues *AtrbohD* and *AtrbohF* are required for accumulation of reactive oxygen intermediates in the plant defense response. Proc Natl Acad Sci USA. 2002;99:517-522.
76. Yoshioka H, Numata N, Nakajima K, Katou S, Kawakita K, Rowland O, Jones JDG, Doke N. Nicotiana benthamiana gp91^{phox} homologs *NbrbohA* and *NbrbohB* participate in H_2O_2 accumulation and resistance to *Phytophthora infestans*. Plant Cell. 2003;15:706-718.
77. Adachi H, Yoshioka H. Kinase-mediated orchestration of NADPH oxidase in plant immunity. Brief Funct Genomics. 2015;14:253-259.
78. Yamamizo C, Doke N, Yoshioka H, Kawakita K. Involvement of mitogen-activated protein kinase in the induction of *StrbohC* and *StrbohD* genes in response to pathogen signals in potato. J Gen Plant Pathol. 2007;73:304-313.
79. Asai S, Ohta K, Yoshioka H. MAPK signaling regulates nitric oxide and NADPH oxidase-dependent oxidative bursts in *Nicotiana benthamiana*. Plant Cell. 2008;20:1390-1406.

80. Lei J, Zhou J, Sun H, Wan W, Xiao J, Yuan C, Karafiátová M, Doleel J, Wang H, Wang X. Development of oligonucleotide probes for FISH karyotyping in *Haynaldia villosa*, a wild relative of common wheat. The Crop J. 2020;8:676-681.
81. Tang Z, Yang Z, Fu S. Oligonucleotides replacing the roles of repetitive sequences pAs1, pSc119.2, pTa-535, pTa 71, CCS1, and PAWRC.1 for FISH analysis. J Appl Genet. 2014;55:313-318.
82. Dai Y, Tabassum MA, Chen L, Pan Z, Song L. Physiological and transcriptomic response of soybean seedling roots to variable nitrate levels. Agronomy J. 2021;113:3639-3652.

Figures

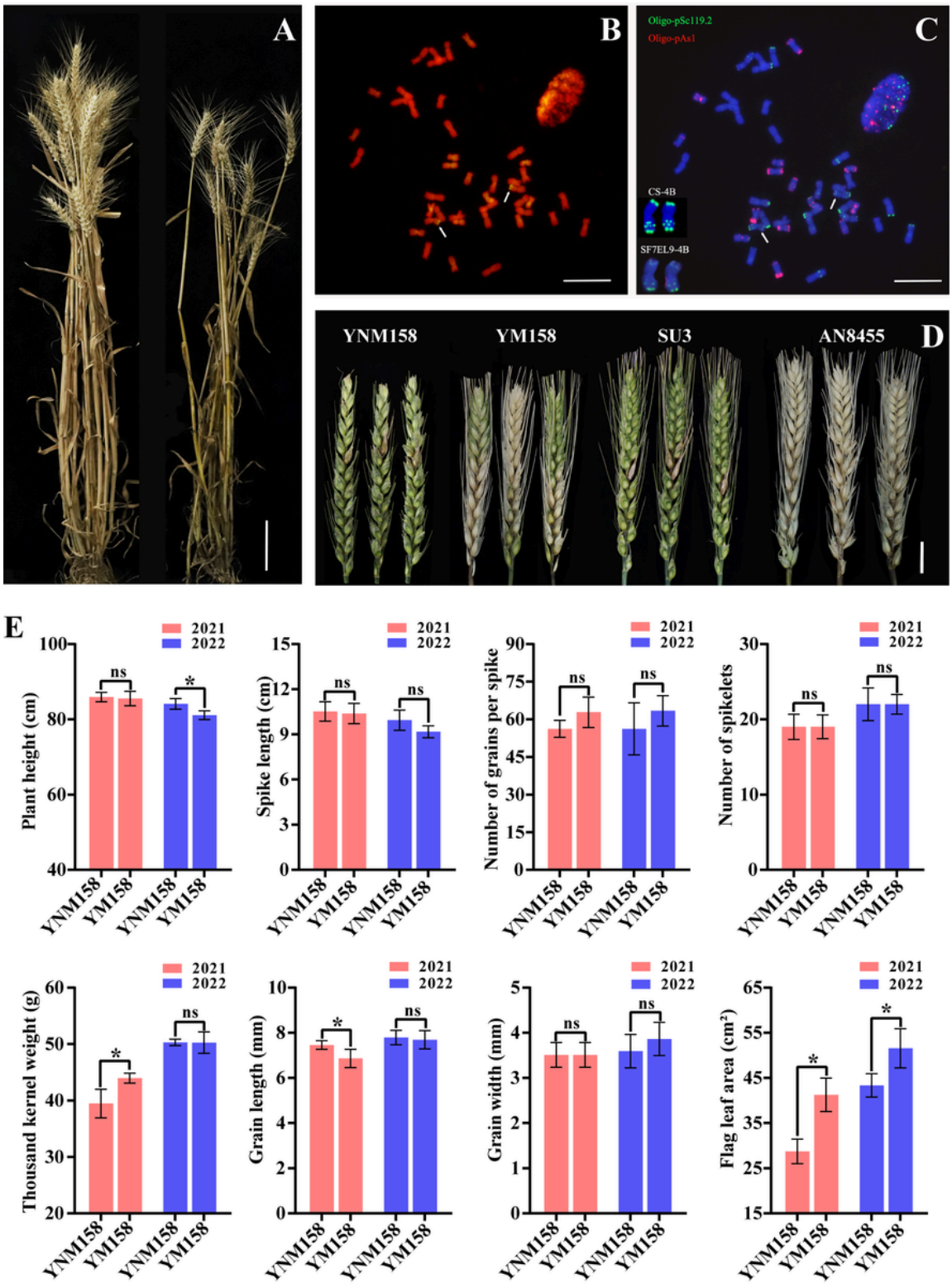

Figure 1

The establishment of wheat-*Th. elongatum* 7EL chromosome translocation line YNM158. (A) Mature plants of YNM158 (left) and YM158 (right). Scale bar = 10 cm. (B) GISH analysis of the translocation lines YNM158, diploid *Th. elongatum*genomic DNA was used as a probe (green). Arrows show the translocated chromosome pair. Scale bar = 100 μm. (C) ND-FISH analysis of the translocation lines YNM158, Oligo-pAs1 (red signal) modified with 5'TAMRA and Oligo-pSc119.2 (green signal) modified

with 5'FAM were used as probes. Chromosomes were counterstained with DAPI (blue). Arrows show the translocated chromosome pairs. Scale bar = 100 μm. (D) Symptoms of YNM158 and the control varieties at 21 dpi with *F. graminearum* isolate F0609. Scale bar = 2 cm. Statistical analysis of eight agronomic traits for YNM158 and YM158. Statistical significance of differences was evaluated by t-test (*, $P < 0.05$, ***, $P < 0.01$)

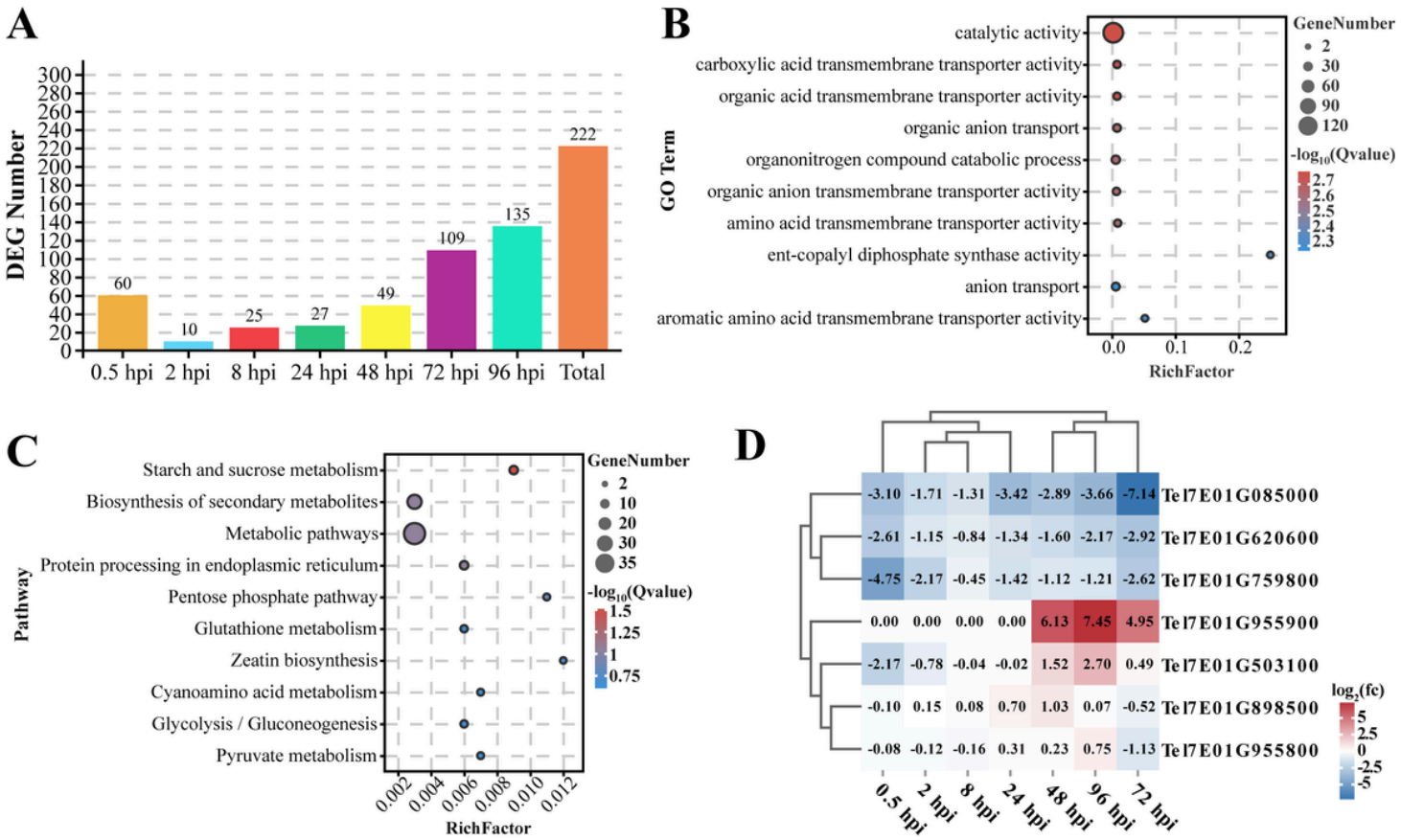

Figure 2

Analysis of the differentially expressed genes (DEGs) identified from YNM158. (A) Statistical analysis of the DEGs number on 7EL chromosome at different time after *F. graminearum* infection. (B) Gene ontology function enrichment analysis of DEGs on 7EL chromosome after *F. graminearum* infection. (C) KEGG pathway enrichment analysis of DEGs on 7EL chromosome after *F. graminearum* infection. (D) The heatmap of the DEGs enriched in starch and sucrose metabolism pathway.

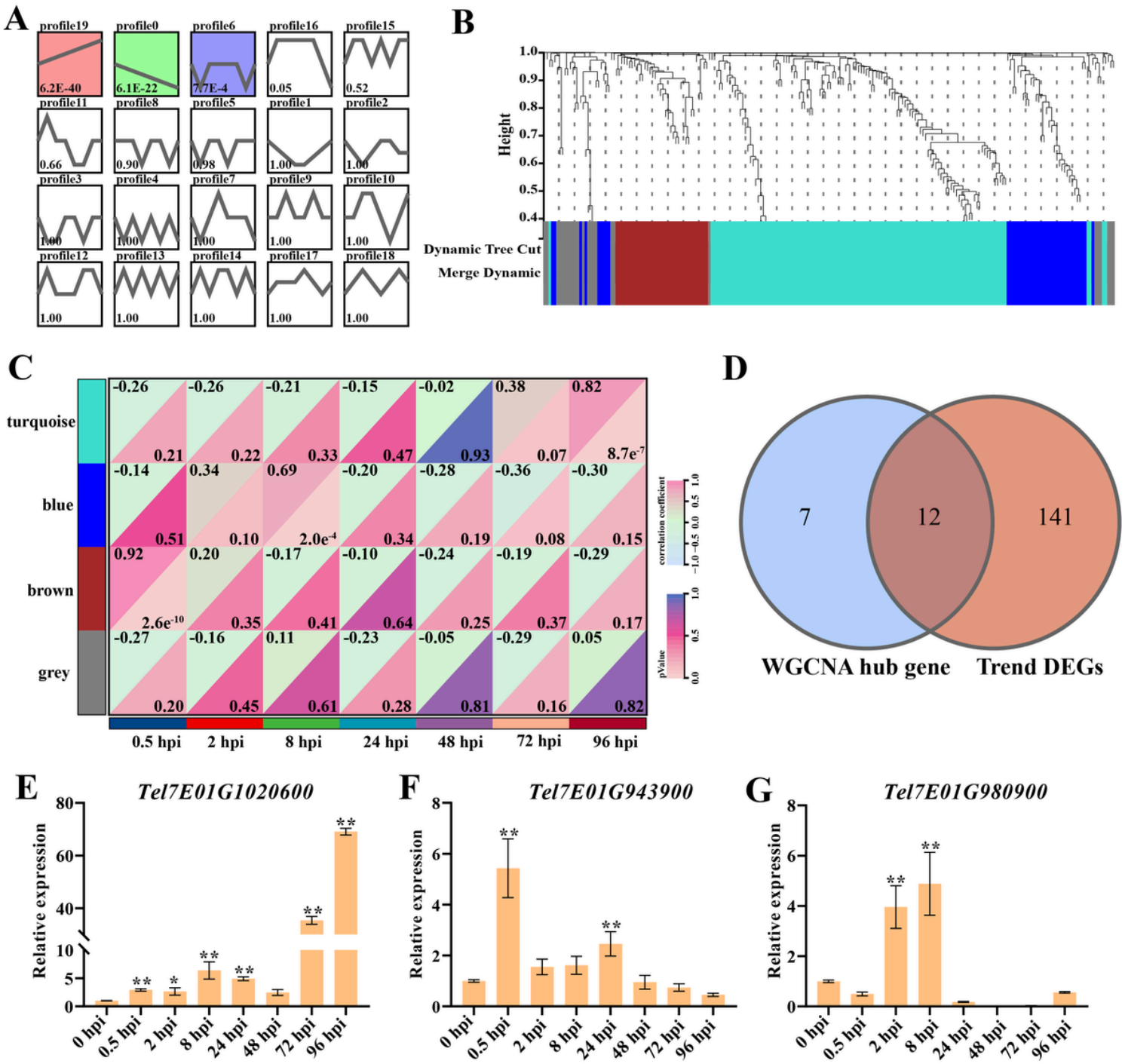

Figure 3

Gene expression patterns analysis on 7EL chromosome. (A) The trend analysis of DEGs at different times after *F. graminearum* infection. (B) Gene dendrogram by clustering the dissimilarity based on topological overlap. (C) Correlation heatmap between modules and infection time with *F. graminearum*. The 4 modules are provided in the left panel. The module-trait correlation, from -1 (light blue) to 1 (pink), is indicated with the color scale on the right. Each column presents the infection time, and their association with each module is represented by a correlation coefficient (showing top left corner) and a *P*-value (showing lower right corner). (D) Venn diagrams showing the overlapping of DEGs between WGCNA and trend analysis. (E-G) Relative expression of *Tel7E01G1020600*, *Tel7E01G946300* and

Tel7E01G980900 by qRT-PCR. (H) The correlation analysis between the relative expression obtained by qRT-PCR and RNA-seq by Pearson correlation analysis. *, $P < 0.05$, ***, $P < 0.01$ by Student's t-test.

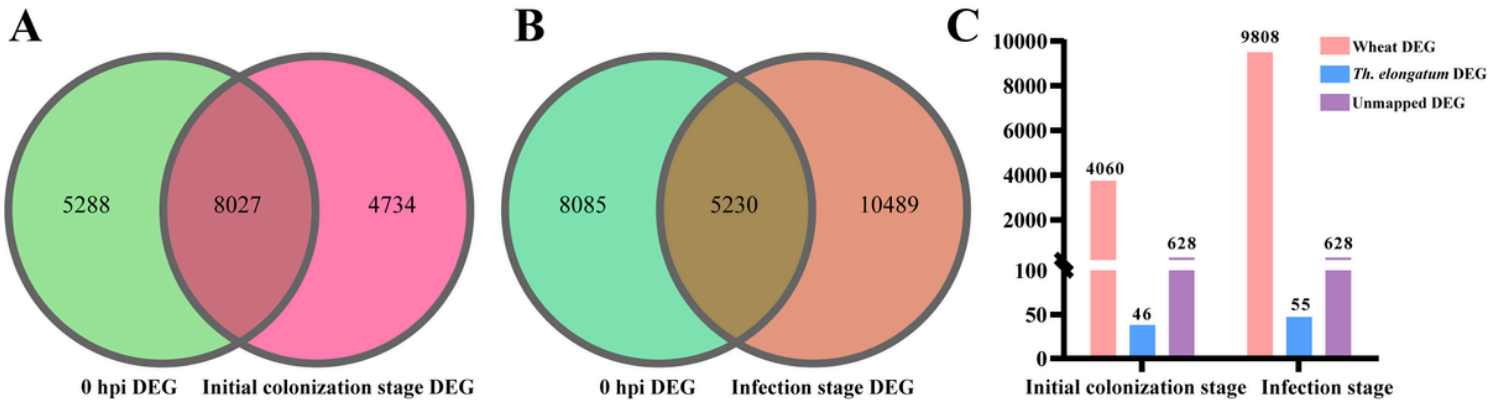

Figure 4

Screened the DEGs between YM158 and YNM158. (A) DEGs Venn diagram of initial colonization stage. (B) DEGs Venn diagram at infection stage. (C) Different types of specific DEGs statistics.

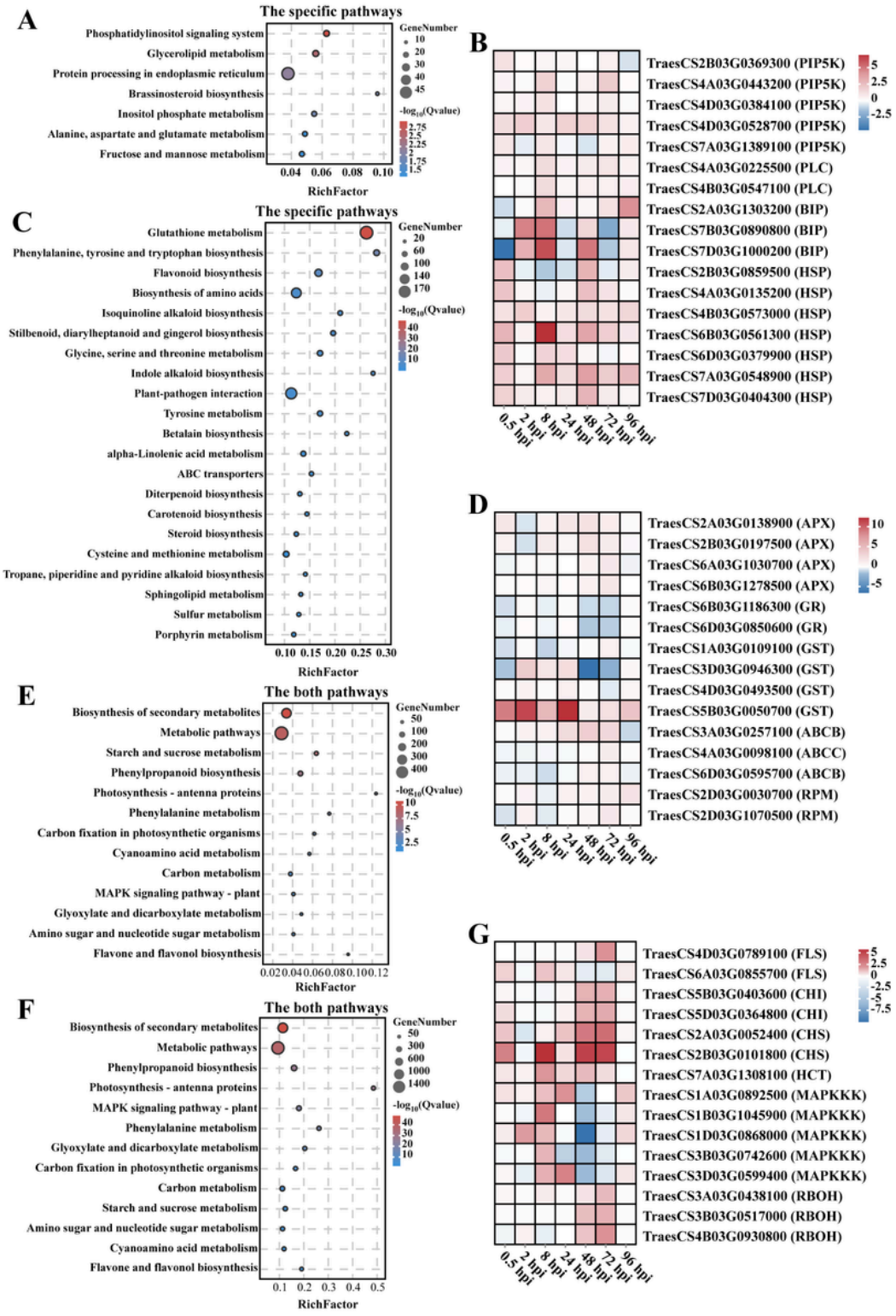

Figure 5

KEGG pathway enrichment analysis of wheat DEGs. (A) The specific enrichment pathways at initial colonization stage. (B) The heatmap of the representative DEGs enriched at initial colonization stage. (C) The specific enrichment pathways at infection stage. (D) The heatmap of the representative DEGs enriched at infection stage. (E) The same enrichment pathways at initial colonization stage. (F) The

same enrichment pathways at infection stage. (G) The heatmap of the representative DEGs enriched at both stages.

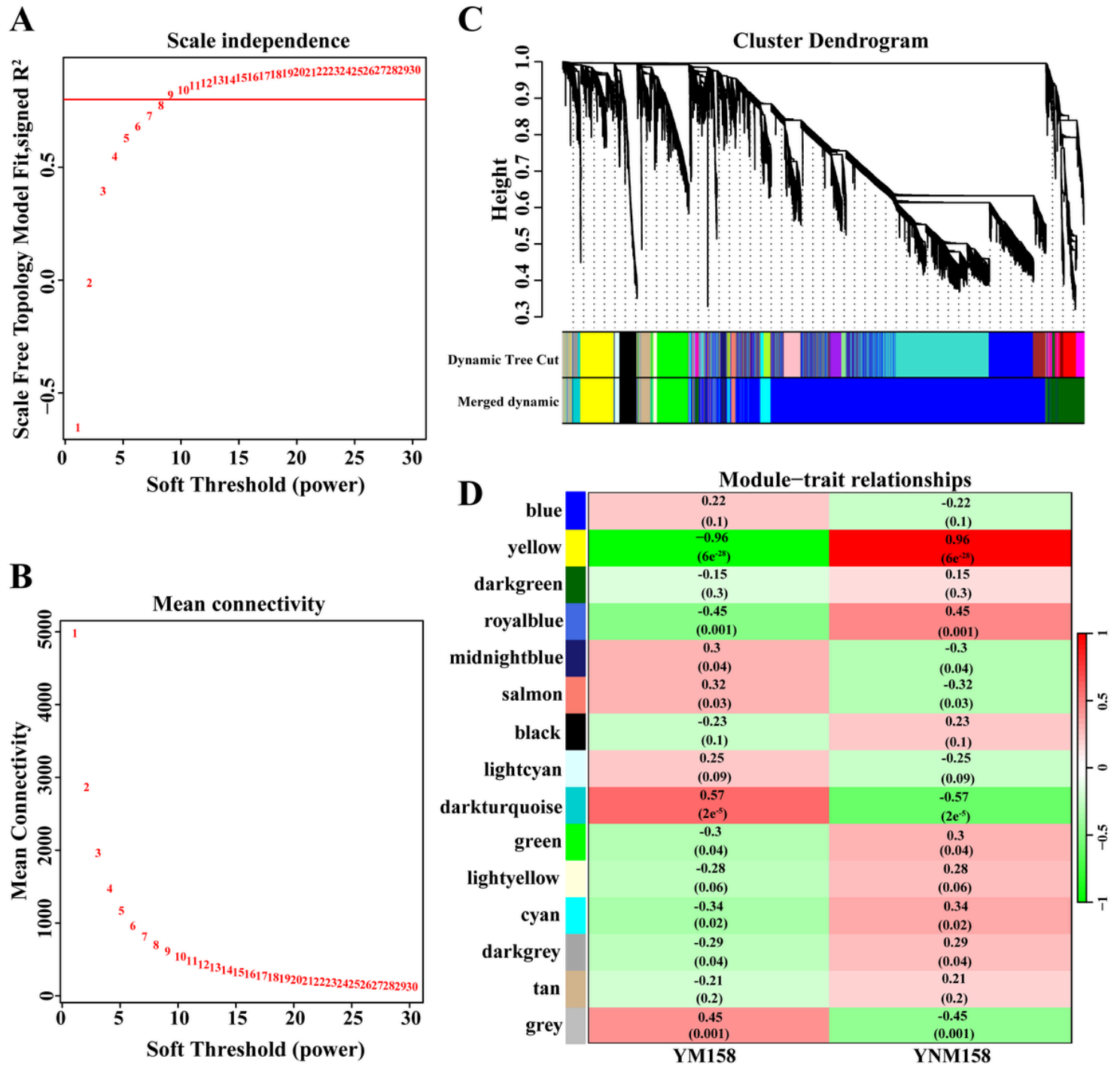

Figure 6

WGCNA of wheat DEGs identified in the YM158 and YNM158 after *F. graminearum* infection. (A) The x-axis represents the soft threshold β. (B) The y-axis represents the mean of all gene's adjacency functions in the corresponding gene module.(C) Fourteen modules of co-expressed genes are shown in a hierarchical cluster tree. A major tree branch represents a module. Modules in designated colors are presented in the lower panel. (D) Module-trait relationships. The 14 modules are provided in the left panel. The module-trait correlation, from -1 (green) to 1 (red), is indicated with the color scale on the

right. The association with each module is represented by a correlation coefficient and a *P*-value (showing in parentheses).

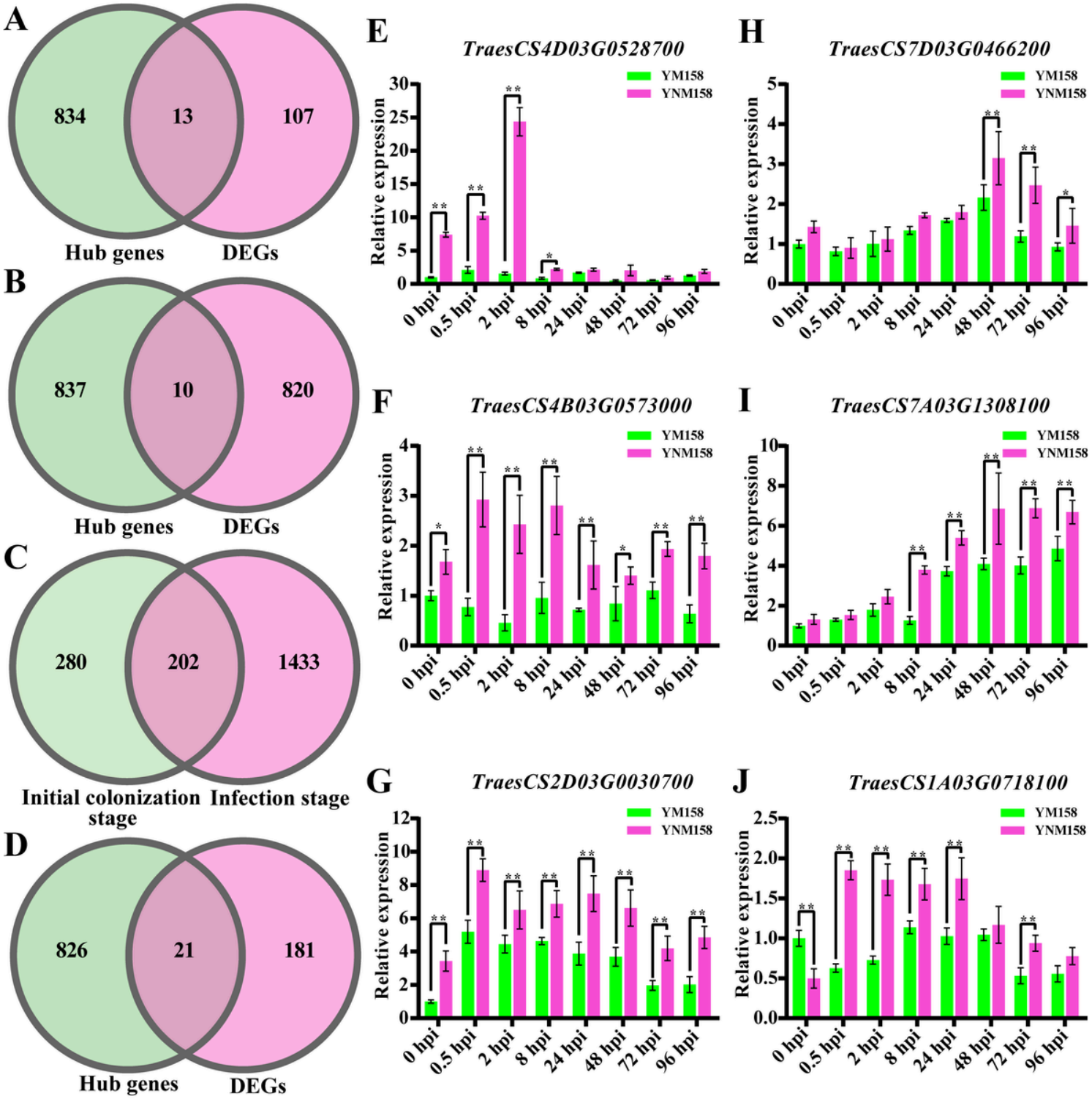

Figure 7

The core genes extraction and expression verification by RT-PCR. (A) Venn diagram between the hub genes associated with YNM158 and DEGs in the specific pathways at initial colonization stage. (B) Venn diagram between the hub genes associated with YNM158 and DEGs in the specific pathways at infection stage. (C) DEGs Venn diagram between initial colonization stage and infection stage in the same

pathways. (E-J) The relative expression of the core genes in YM158 and YNM158. *, $P < 0.05$, ***, $P < 0.01$ by Student's t-test.

Supplementary Files

This is a list of supplementary files associated with this preprint. Click to download.

- Additionalfile1.doc
- Additionalfile2.xls